

Hyperoside Inhibits High-Glucose-Induced Vascular Inflammation *In Vitro* and *In Vivo*

Sae-Kwang Ku,¹ Soyoung Kwak,² O-Jun Kwon,³ and Jong-Sup Bae^{2,4}

Abstract—Hyperoside, an active compound from the genera of *Hypericum* and *Crataegus*, was reported to have antioxidant, antihyperglycemic, anticancer, anti-inflammatory, and anticoagulant activities. Vascular inflammatory process has been suggested to play a key role in initiation and progression of atherosclerosis, a major complication of diabetes mellitus. Thus, in this study, we attempted to determine whether hyperoside can suppress vascular inflammatory processes induced by high glucose (HG) in human umbilical vein endothelial cells (HUVECs) and mice. Data showed that HG induced markedly increased vascular permeability, monocyte adhesion, expressions of cell adhesion molecules (CAMs), formation of reactive oxygen species (ROS), and activation of nuclear factor (NF)- κ B. Remarkably, all of the above-mentioned vascular inflammatory effects of HG were attenuated by pretreatment with hyperoside. Vascular inflammatory responses induced by HG are critical events underlying development of various diabetic complications; therefore, our results suggest that hyperoside may have significant therapeutic benefits against diabetic complications and atherosclerosis.

KEY WORDS: hyperoside; high glucose; diabetes mellitus; inflammation; atherosclerosis.

INTRODUCTION

Diabetes mellitus is an endocrine disorder that is characterized by hyperglycemia resulting from a defect in insulin secretion, insulin action, or both [1], and hyperglycemia is one of the major risk factors in the development of atherosclerotic heart diseases [2]. Diabetes is a major threat to global public health that is rapidly getting worse and has the biggest impact on adults of working age in developing countries [3]. Although diabetes is often not recorded as the cause of death, globally, it is believed to be the fifth leading cause of death in 2000 after communicable diseases, cardiovascular disease, cancer, and injuries [4]. There are an estimated 366 million people with diabetes

in the world, of whom about 80 % reside in developing countries, and this is expected to rise to 552 million by 2030 [1]. The number of cases of non-insulin-dependent diabetes mellitus (type 2) has increased dramatically due to the changes in lifestyle, increasing prevalence of obesity, and aging of populations. The most disturbing trend is a shift in age of onset of diabetes to a younger age in recent years [1]. It can be managed by exercise, diet, and chemotherapy. In modern medicine, no satisfactory effective therapy is still available to cure diabetes mellitus [5]. However, the pharmaceutical drugs are either too expensive or have undesirable side effects or contraindications [6]. Therefore, the search for more effective and safer hypoglycemic agents has continued to an area of active research. Many indigenous medicinal plants have been found to be useful to successfully manage diabetes, and some of them have been tested and their active ingredients isolated [7]. The World Health Organization (WHO) has also recommended the evaluation of the plants' effectiveness and conditions where we lack safe modern drugs [8].

The search for anti-inflammatory agents from natural herbal medicines has attracted considerable interest [9]. After screening several dozen of commonly used herbs, we found that compounds from herbal medicines efficiently exhibited anti-inflammatory responses [10]. Flavonoids

¹Department of Anatomy and Histology, College of Korean Medicine, Daegu Haany University, Gyeongsan, 712-715, Republic of Korea

²College of Pharmacy, CMRI, Research Institute of Pharmaceutical Sciences, Kyungpook National University, 80 Dahak-ro, Buk-gu, Daegu 702-701, Republic of Korea

³Daegyeong Institute for Regional Program Evaluation, Gyeongsan, 712-210, Republic of Korea

⁴To whom correspondence should be addressed at College of Pharmacy, CMRI, Research Institute of Pharmaceutical Sciences, Kyungpook National University, 80 Dahak-ro, Buk-gu, Daegu 702-701, Republic of Korea. E-mail: baejs@knu.ac.kr

are naturally occurring low molecular weight and polyphenolic compounds distributed in fruits, vegetables, plants, and plant-based foods that possess potent biological effects including cytoprotective, antioxidant, antiplatelet, antithrombotic, and anticarcinogenic activities [11, 12]. Flavonoids display a variety of anti-inflammatory properties, some of which are suggested to affect the function of immune system [13]. Hyperoside is a flavonol glycoside mainly found in the genera of *Hypericum* and *Crataegus* [14]. Pharmacological investigation demonstrated that hyperoside had a variety of biological activities, such as antioxidant [15], antihyperglycemic [16], anticancer [17], anti-inflammatory [18], and cardioprotective activities [19]. Recently, we reported that hyperoside was reported to have an anticoagulant effect [20]. However, no studies on high-glucose-induced inflammatory responses of hyperoside have been reported. Therefore, in the current study, we attempted to determine whether hyperoside could suppress the vascular inflammatory process induced by high glucose (HG) in primary-cultured human endothelial cells and in mice.

MATERIALS AND METHODS

Reagents

Hyperoside, rutin, quercetin, quercitrin, D-glucose, L-glucose, D-mannitol, Evans blue, 2-mercaptoethanol, and antibiotics (penicillin G and streptomycin) were purchased from Sigma (St. Louis, MO, USA). Fetal bovine serum (FBS) and Vybrant DiD were purchased from Invitrogen (Carlsbad, CA, USA).

Cell Culture

Primary human umbilical vein endothelial cells (HUVECs) were obtained from Cambrex Bio Science (Charles City, IA, USA) and maintained as described previously [21]. Briefly, the cells were cultured to confluency at 37 °C and 5 % CO₂ in EBM-2 basal media supplemented with growth supplements (Cambrex Bio Science). THP-1 cells, a monocyte cell line, were maintained as previously described [22].

Animals and Husbandry

Male C57BL/6 mice (6–7-week-old, weighting 18–20 g) purchased from Orient Bio Co. (Sungnam, Kyungki-do, Republic of Korea) were used in this study after a 12-day acclimatization period. The animals were housed five

per polycarbonate cage under controlled temperature (20–25 °C) and humidity (40–45 %) and a 12:12 hour light/dark cycle. The animals were supplied a normal rodent pellet diet and water *ad libitum* during acclimatization. All animals were treated in accordance with the Guidelines for the Care and Use of Laboratory Animals issued by Kyungpook National University.

Cell Viability Assay

Microculture tetrazolium test (MTT) was used as an indicator of cell viability. Cells were grown in 96-well plates at a density of 5×10^3 cells/well. After 24 h, the cells were washed with fresh medium, followed by treatment with hyperoside. After a 48-h incubation period, the cells were washed, and 100 μ l of MTT (1 mg/ml) was added, followed by incubation for 4 h. Finally, DMSO (150 μ l) was added in order to solubilize the formazan salt formed, and the amount of formazan salt was determined by measuring the OD at 540 nm using a microplate reader (Tecan Austria GmbH, Austria).

Permeability Assay *In Vitro*

Endothelial cell permeability in response to increasing concentrations of hyperoside was quantified by spectrophotometric measurement of the flux of Evans blue dye-bound albumin across functional cell monolayers using a modified two-compartment chamber model. HUVECs were plated (5×10^4 /well) in 3- μ m pore size, 12-mm diameter Transwell inserts for 3 days. Confluent monolayers were incubated with increasing concentrations of hyperoside for 6 h followed by incubation with indicated concentrations of HG for 24 h. Then, the Transwell inserts were washed with phosphate-buffered saline (PBS) (pH 7.4), followed by addition of 0.5 ml of Evans blue (0.67 mg/ml) diluted in growth medium containing 4 % bovine serum albumin (BSA). Fresh growth medium was then added to the lower chamber, and the medium in the upper chamber was replaced with Evans blue/BSA. Ten minutes later, optical density was measured at 650 nm in the lower chamber.

Permeability Assay *In Vivo*

Mice were pretreated with intravenous administration of hyperoside (18.6 or 46.4 μ g/mouse), and after 6 h, 1 % Evans blue dye solution in normal saline was administered by intravenous injection in each mouse immediately followed by an intravenous injection of HG (9 mg/kg). Thirty minutes later, the mice were sacrificed, and the

peritoneal exudates were collected after being washed with 5 ml of normal saline and centrifuged at $200\times g$ for 10 min. The absorbance of the supernatant was read at 650 nm. Vascular permeability was expressed in terms of dye ($\mu\text{g}/\text{mouse}$), which leaked into the peritoneal cavity according to a standard curve of Evans blue dye, as previously described [23, 24].

Expression of Cell Adhesion Molecules (CAMs)

Expression of vascular cell adhesion molecule-1 (VCAM-1), intercellular adhesion molecule-1 (ICAM-1), and E-selectin was determined by whole-cell enzyme-linked immunosorbent assay (ELISA). Briefly, HUVEC monolayers were treated with hyperoside at the indicated concentrations for 6 h, followed by treatment with HG (25 mM) for 24 h, and fixed in 1 % paraformaldehyde. After washing three times, mouse antihuman monoclonal antibodies (VCAM-1, ICAM-1, and E-selectin; Temecula, CA, USA, 1:50 each) were added, and cells were incubated for 1 h (37°C , 5 % CO_2). The cells were then washed, treated with peroxidase-conjugated anti-mouse IgG antibody (Sigma, St. Louis, MO) for 1 h, washed three times, and then developed using *o*-phenylenediamine substrate (Sigma, St. Louis, MO). All measurements were performed in triplicate wells.

Cell-Cell Adhesion Assay

Adherence of monocytes to endothelial cells was evaluated by fluorescent labeling of monocytes. Briefly, monocytes were labeled with $5\text{-}\mu\text{M}$ Vybrant DiD for 20 min at 37°C in phenol red-free RPMI containing 5 % fetal bovine serum. Following two washing steps, the cells ($1.5\times 10^6/\text{ml}$, $200\ \mu\text{l}/\text{well}$) were resuspended in adhesion medium (RPMI containing 2 % fetal bovine serum and 20 mM 4-(2-hydroxyethyl)-1-piperazineethanesulfonic acid (HEPES)) and added to confluent monolayers of HUVECs in 96-well plates, which were treated for 6 h with hyperoside followed by HG (25 mM for 24 h). Fluorescence of labeled cells was measured (total signal) using a fluorescence microplate reader (Tecan Austria GmbH, Austria). After incubation for 1 h at 37°C , non-adherent cells were removed by washing four times with prewarmed RPMI, and the fluorescent signals of adherent cells were measured using the previously described methods. The percentage of adherent monocytes was calculated using the formula: $\% \text{adherence} = (\text{adherent signal}/\text{total signal})\times 100$ as described [25, 26].

RNA Preparation and Real Time qRT-PCR

HUVECs were grown in six-well plates and incubated with hyperoside for 6 h, followed by HG 25 mM for 24 h. The High Pure RNA Isolation Kit, from Roche Diagnostics, was used for the isolation of RNA from cell cultures, and RNA quality was tested by measuring the ratio 260:280 nm in a UV spectrophotometer. For each sample, $0.5\ \mu\text{g}$ of total RNA was reverse transcribed into complementary DNA (cDNA) using the Transcriptor First Strand cDNA Synthesis Kit (Roche Diagnostics).

Real-time PCR analysis was performed using the LightCycler[®] 96 System (Roche Diagnostics, Mannheim, Germany) using FastStart Essential DNA Green Master (Roche Diagnostics) according to the manufacturer's instructions. Glyceraldehyde 3-phosphate dehydrogenase (GAPDH) was used as an internal control. The relative quantification of messenger RNA (mRNA) expression was calculated as a ratio of the target gene to GAPDH. Specific sense and antisense primers used were as follows, respectively: monocyte chemoattractant protein-1 (MCP-1), sense: 5'-TGCAGAGGCTCGCGAGCTA-3', antisense: 5'-CAGGTGGTCCATGGAATCCTGA-3'; IL-8, sense: 5'-ACTGAGAGTGATTGAGAGTGGAC-3', antisense: 5'-AACCCCTCTGCACCCAGTTTTTC-3'; GAPDH, sense: 5'-GTCTTCACTACCATGGAGAAGG-3', antisense: 5'-TCATGGATGACCTTGCCAG-3'.

H₂O₂ Release Assay

Extracellular production of H₂O₂ was quantified using the Amplex Red Hydrogen Peroxide Assay Kit (Molecular Probes; Eugene, OR, USA) according to the manufacturer's recommendations. The cells were washed twice with an ice-cold PBS and harvested by microcentrifugation and resuspended in a Krebs-Ringer phosphate glucose (KRP) solution; $100\ \mu\text{l}$ of the reaction mixture ($50\text{-}\mu\text{M}$ Amplex Red reagent containing 0.1 U/ml HRP in KRP) was added to each microplate well and then prewarmed at 37°C for 10 min. Then, the reaction was started by the addition of the resuspended cells in $20\ \mu\text{l}$ of KRP. Fluorescence readings became stable within 30 min of starting the reaction equipped for absorbance at $\sim 560\ \text{nm}$ (Multiskan, Thermo Labsystems Inc, Franklin, MA, USA). A reagent H₂O₂ standard curve was used for the calculation of H₂O₂ concentration.

Preparation of Cytoplasmic and Nuclear Extracts

The cells were harvested rapidly by sedimentation, and nuclear and cytoplasmic extracts were prepared on ice,

as previously described [27]. The cells were harvested and washed with 1-ml buffer A (10 mM HEPES, pH 7.9, 1.5 mM MgCl₂, 19 mM KCl) for 5 min at 600g. The cells were resuspended in buffer A and then centrifuged at 600g for 3 min, resuspended in 30- μ l buffer B (20 mM HEPES, pH 7.9, 25 % glycerol, 0.42 M NaCl, 1.5 mM MgCl₂, 0.2 mM EDTA), rotated for 30 min at 4 °C, and then centrifuged at 13,000g for 20 min. The supernatant was used as a nucleus extract. The nucleus and cytosolic extracts were then analyzed for protein content using Bradford assay.

Western Blotting

Total cell extracts were prepared by lysing the cells, and protein concentration was determined using the Bradford assay methods. Equal amounts of protein were separated by SDS-PAGE (10 %) and electroblotted overnight onto an Immobilon membrane (Millipore, Billerica, MA, USA). The membranes were blocked for 1 h with 5 % low-fat milk-powder TBS (50 mM Tris-HCl, pH 7.5, 150 mM NaCl) containing 0.05 % Tween 20 and then incubated with NF- κ B p65 for 1.5 h at room temperature (1:1000, Santa Cruz, CA, USA), followed by incubation with horseradish-peroxidase-conjugated secondary antibody and ECL detection according to the manufacturer's instructions.

Immunofluorescence Staining

HUVECs were grown to confluence on glass cover slips coated with 0.05 % Poly-L-Lysine in complete media containing 10 % FBS and maintained for 48 h. The cells were then stimulated with HG (25 mM) for 1 h with or without prior treatment with hyperoside for 2 h. After several washes with PBS, the cells were fixed in 4 % formaldehyde in PBS (v/v) for 15 min at room temperature, and for immunostaining, the cells were permeabilized in 0.05 % Triton X-100 in PBS for 15 min and blocked in a blocking buffer (5 % BSA in PBS) overnight at 4 °C. The cells were incubated with primary rabbit monoclonal NF- κ B p65 antibody, anti-rabbit Alexa 488, overnight at 4 °C. Nuclei were counterstained with 4,6-diamidino-2-phenylindole dihydrochloride (DAPI). The cells were then visualized by confocal microscopy at a \times 63 magnification (TCS-SP5, Leica Microsystems, Germany).

PHARMACOKINETIC PARAMETERS

After an intravenous penile vein injection of male C57BL/6 mice with each flavonoid at 5 mg/kg,

approximately 100 μ l of blood was obtained from the tail vein or oral administration immediately before and 5, 15, 30, 60, and 180 min after the administration of the dose. Following the addition of 80 μ l acetonitrile and internal standard solution (reserpine), 10- μ l plasma samples were prepared by centrifugation of the blood at 13,000 rpm for 15 min at 4 °C; 2- μ l supernatants were then injected into a high-performance liquid chromatography (HPLC) column. The pharmacokinetic parameters were determined using the standard non-compartmental method. Serum AUC was calculated using WinNonlin (version 2.0, Scientific Consulting, KY, USA) with a log-linear trapezoidal method.

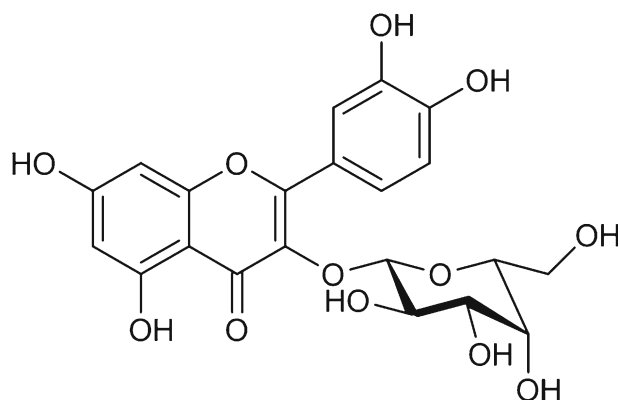
The samples were analyzed using an Accela™ LC system coupled to a TSQ Vantage triple quadrupole mass spectrometer (Thermo Fisher Scientific Inc., USA) equipped with a HESI-II Spray source. An ACE® 5C18 3- μ m (2.1 \times 50 mm, ACE) column was used for the liquid chromatography (LC) analysis. The mobile phases consisted of LC grade® water containing 0.1 % formic acid (A) and LC grade acetonitrile containing 0.1 % formic acid (B). The initial composition was increased to 95 % solvent (B) for 3 min. A gradient program was used for HPLC at a flow rate of 230 ml/min. Electrospray ionization was performed in a positive mode at a spray voltage of 3,500 V. Nitrogen was used as the sheath and auxiliary gas at optimum values of 45 and 20 (arbitrary units), respectively. Vaporizer and capillary temperatures were 150 and 300 °C, respectively. Multiple reaction monitoring (MRM) detection was employed using nitrogen as the collision as each transition monitored was 479 \rightarrow 317 for isorhamnetin 3-O-galactoside, 465 \rightarrow 303 for hyperoside, and 609 \rightarrow 174 for reserpine (IS).

Statistical Analysis

Results are expressed as mean \pm standard error of mean (SEM) of at least three independent experiments. Statistical significance was determined using the analysis of variance (ANOVA; SPSS, version 14.0, SPSS Science, Chicago, IL, USA), and *p* values less than 0.05 (*p* < 0.05) were considered significant.

RESULTS AND DISCUSSION

In this study, the effects of hyperoside (Hyp, Fig. 1) on HG-induced vascular inflammation were determined *in vitro* and *in vivo*. The pharmacokinetic values in plasma of hyperoside are shown in Table 1.



Hyperoside (Hyp)

Fig. 1. Structure of hyperoside.

Effects of Hyperoside on HG-Induced Disruption of the Endothelial Barrier Function of HUVECs and in Mice

Previous evidence has suggested that endothelial dysfunction and damage are the early steps in the pathophysiology of vascular complications in diabetes mellitus [28]. Hyperglycemia is the central-initiating factor for all types of diabetic microvascular disease, and it may also be involved in the pathogenesis of macrovascular complications [28–30]. In addition, endothelial cell permeability is impaired in diabetes mellitus and may be increased by high concentrations of extracellular glucose [31]. Leakage of serum proteins, particularly albumin, through the endothelium is observed in retinal vessels early in diabetes mellitus [31, 32]. Increased endothelial cell permeability in larger vessels leads to the development of interstitial edema and may result in enhancement of cell proliferation and matrix production [30]. Therefore, we first investigated the effects of glucose on the albumin permeability of endothelial cells, as shown in Fig. 2a. Treatment with HG (25 and 50 mM) led to a rapid increase in endothelial cell permeability (Fig. 2a). This effect began from 12 h after incubation

and reached its maximum at 24 h (Fig. 2b). A significant increase was observed at a glucose concentration of 10 mM. Concentrations above 50 mM did not further increase the glucose-induced permeability (data not shown). L-glucose and D-Mannose (25 mM), which were used as an osmotic control, had no significant effect on endothelial cell permeability (Fig. 2a).

Next, we attempted to determine whether hyperoside could alter HG-induced hyperpermeability. Treatment with 50 μ M hyperoside alone did not result in alteration of barrier integrity (Fig. 2c). As shown in Fig. 2c, treatment with hyperoside resulted in a dose-dependent decrease in HG-mediated membrane disruption. To confirm this vascular barrier protective effect *in vivo*, HG-mediated vascular permeability in mice was assessed. As shown in Fig. 2d, treatment with hyperoside resulted in markedly inhibited peritoneal leakage of dye induced by HG. Assuming that the average weight of a mouse was 20 g and the average blood volume was 2 ml, the amount of hyperoside injected (4.6, 9.3, 18.6, or 46.4 μ g per mouse) was equivalent to 5, 10, 20, or 50 μ M in peripheral blood. To test the effects of cellular viability of hyperoside, MTT assays were performed in HUVECs treated with hyperoside for 24 h. At the concentrations used (up to 50 μ M), hyperoside did not affect cell viability (Fig. 2e). These findings demonstrate inhibition of HG-mediated endothelial disruption and maintenance of human endothelial cell barrier integrity by hyperoside in mice treated with HG. Therefore, prevention of HG-induced hyperpermeability by hyperoside suggests the potential of hyperoside in the treatment of vascular inflammatory diseases.

Effects of Hyperoside on HG-Mediated Expression of CAMs and THP-1 Adhesion

The two key early events in pathogenesis of atherosclerosis are the adhesion of monocytes to the endothelium followed by the transmigration into the subendothelial space and enhanced vascular cellular permeability [31, 33]. Increased leukocyte-endothelial interactions with monocytes from *in vivo* and *in vitro* diabetes models have been demonstrated [33, 34]. Of particular importance, the hyperglycemia/HG-induced augmentation of leukocyte adhesion to the endothelium through upregulation of cell surface expression of CAMs and transendothelial migration (TEM) has been reported to be dependent on NF- κ B activation [35, 36]. In addition, CAMs are believed to

Table 1. Pharmacokinetic Parameters of Hyperoside After Administration of 5 mg/kg ($N=5$)

Parameters	Intravenous injection	Oral (per os)
AUC (μ g h/ml)	15.2	1.7
Half-life (h)	1.6	1.2
C_{max}	7.88 μ g/ml (16.98 μ M)	2.51 μ g/ml (5.41 μ M)

AUC area under curve

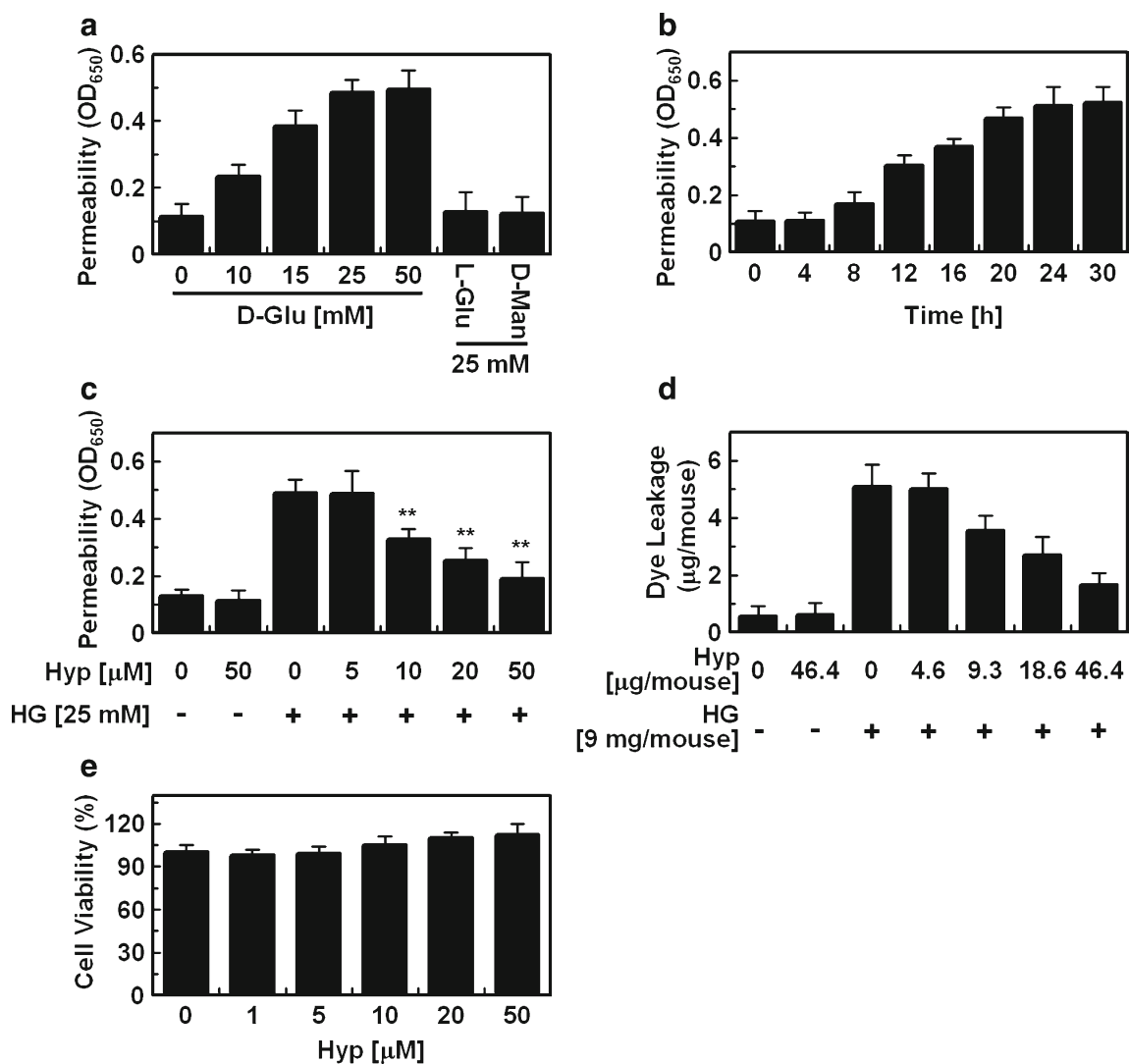


Fig. 2. Effects of hyperoside on HG-mediated permeability *in vitro* and *in vivo*. **a** HUVECs were treated with D-glucose (0–50 mM), L-glucose (25 mM), and D-mannitol (25 mM) for 24 h, and permeability was monitored by measuring the flux of Evans blue-dye-bound albumin across the HUVECs. **b** HUVECs were treated with D-glucose (25 mM) for indicated time periods, and permeability was monitored. **c** The effects of pretreatment with different concentrations of hyperoside for 6 h on barrier disruptions caused by 25 mM HG for 24 h. **d** The effects of hyperoside (intravenous (i.v.) injection) on HG-induced (9 mg/mouse, i.v.) vascular permeability in mice were determined by measuring the levels of Evans blue dye in peritoneal washing steps (expressed μg/mouse, $n = 5$). **e** The effects of hyperoside on cellular viability were measured using MTT assays. Results are expressed as the mean \pm SEM of at least three independent experiments. ** $p < 0.01$ versus 0 (a, b) and HG alone (c, d).

participate in the pathogenesis of atherosclerosis [37]. These proteins regulate the interaction between endothelium and leukocytes, and an increase in their expression on the endothelial surface causes increased adhesion of leukocytes, particularly monocytes, which are well known as one of the first steps in the process leading to atheroma [37]. In particular, over-expression of intracellular adhesion molecule-1 (ICAM-1), VCAM-1, and E-selectin in endothelial cells of human

atherosclerotic lesions has been reported [10]. The effects of HG concentrations on expression of CAMs in endothelial cells have been widely investigated. Increase of ICAM-1 has been reported in human aortic endothelial cells cultured in HG [38]; these data are consistent with findings indicating that HG is a potent promoter of leukocyte adhesion to endothelial cells under flow conditions, depending on upregulation of E-selectin, ICAM-1, and VCAM-1

[36]. Furthermore, one of the earliest events in the vascular inflammation process is adhesion of monocytes to the endothelium, which is followed by their infiltration and differentiation into macrophages [39]. This key step is mediated by an interaction between monocytes and molecules expressed on the surface of endothelial cells [39]. These CAMs primarily mediated the adhesion of monocytes specifically found in atherosclerosis lesions of the vascular endothelium [39]. Therefore, we determined the effects of HG on the expression of CAMs and adhesion of monocytes to HUVECs in response to HG. The responses according to the concentration of HG in the expression of CAMs, such as VCAM-1, ICAM-1, and E-selectin, were determined by cell ELISA. Exposure of the primary cultured HUVECs to HG resulted in significantly increased expression of VCAM-1, ICAM-1, and E-selectin after incubation with 25 mM D-glucose; the maximum inhibitory effect of

hyperoside was observed at 50 μ M (Fig. 3a). In addition, in order to explore the effect of hyperoside on endothelial cell-leukocyte interaction, we examined the adhesion of THP-1 cells to HG-activated HUVECs. Control HUVECs showed minimal binding to THP-1 cells; however, adhesion showed a marked increase upon treatment with HG. Pretreatment with hyperoside (10–50 μ M) resulted in a decrease in the number of THP-1 cells adhering to HG-induced HUVECs (Fig. 3b, c). Thus, hyperoside could be used as a therapeutic drug candidate for diabetic vascular inflammation targeting CAMs expression in the prevention of atherosclerotic lesions.

MCP-1 and IL-8 are the chemokines most strongly implicated in the atherogenesis process [40]. MCP-1 is a key mediator of monocyte trafficking and IL-8 is chemotactic for neutrophils [40]. Thus, we measured the effect of hyperoside on HG-induced MCP-1 and IL-8 mRNA levels using real

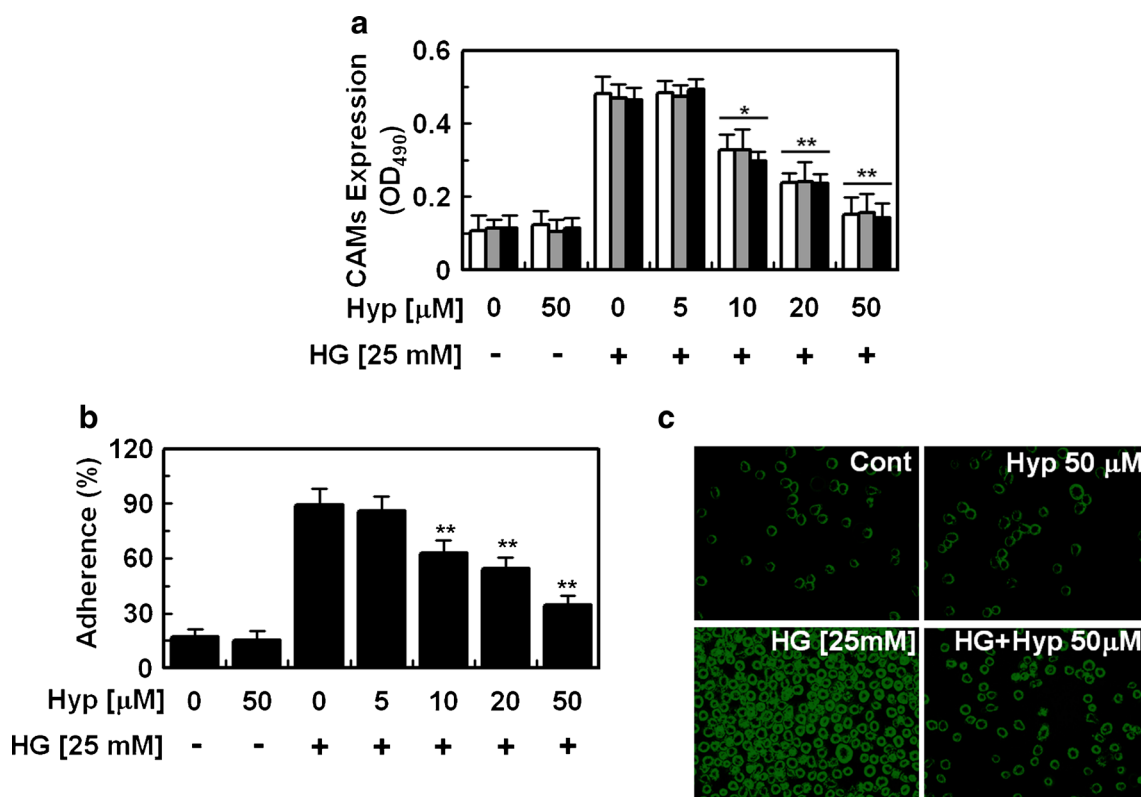


Fig. 3. Effects of hyperoside on HMGB1-mediated pro-inflammatory responses. **a** HG-induced (25 mM, for 24 h) expression of cell adhesion molecules on HUVECs was determined after the treatment of cells with the indicated concentrations of hyperoside for 6 h. VCAM-1 (white bar), ICAM-1 (gray bar), and E-Selectin (black bar) were detected by ELISA. **b, c** HG-induced (25 mM, for 24 h) mediated adherence of monocytes to HUVEC monolayers was assessed after the pretreatment of cells with hyperoside for 6 h. The amounts of adherent THP-1 cells were monitored by **b** cell-cell adhesion assay and **c** fluorescence microscopy. Data are expressed as the mean \pm SEM of three independent experiments. * p <0.05 and ** p <0.01 versus HG alone.

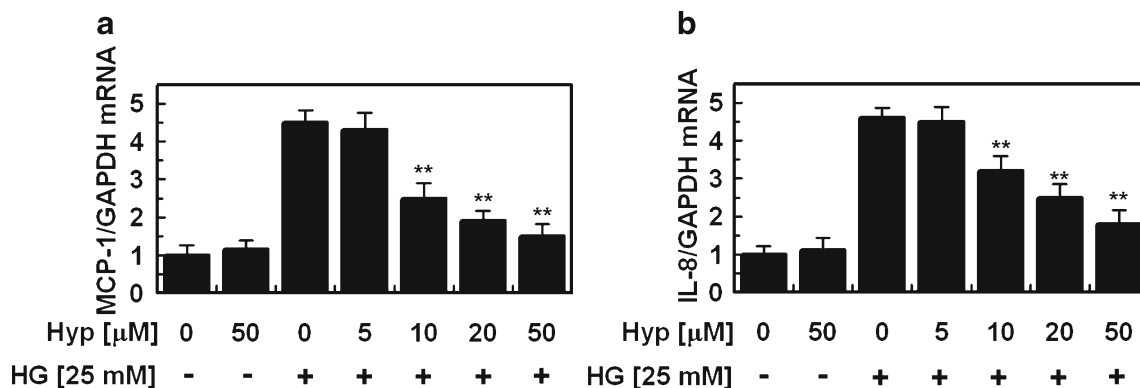


Fig. 4. Effects of hyperoside on HG-induced expression of MCP-1 and IL-8 mRNA in HUVECs. Cells were pretreated with indicated concentrations of hyperoside for 6 h and then incubated with HG (25 mM) for 48 h. The mRNA was extracted, and real-time qRT-PCR analysis was performed using specific primer for MCP-1, IL-8, and GAPDH, as described in the “Materials and Methods” section. Data are expressed as the mean \pm SEM of three independent experiments. $**p < 0.01$ versus HG alone.

time quantitative reverse-transcription (qRT)-PCR. As shown in Fig. 4, HG induced an increase in expression levels of MCP-1 (up to 4.5-fold) and IL-8 (up to 4.6-fold) mRNAs, and pretreatment with hyperoside

resulted in decreased expression levels of HG-induced MCP-1 and IL-8 mRNAs. These results suggested that hyperoside may be useful in the prevention of the vascular inflammatory process.

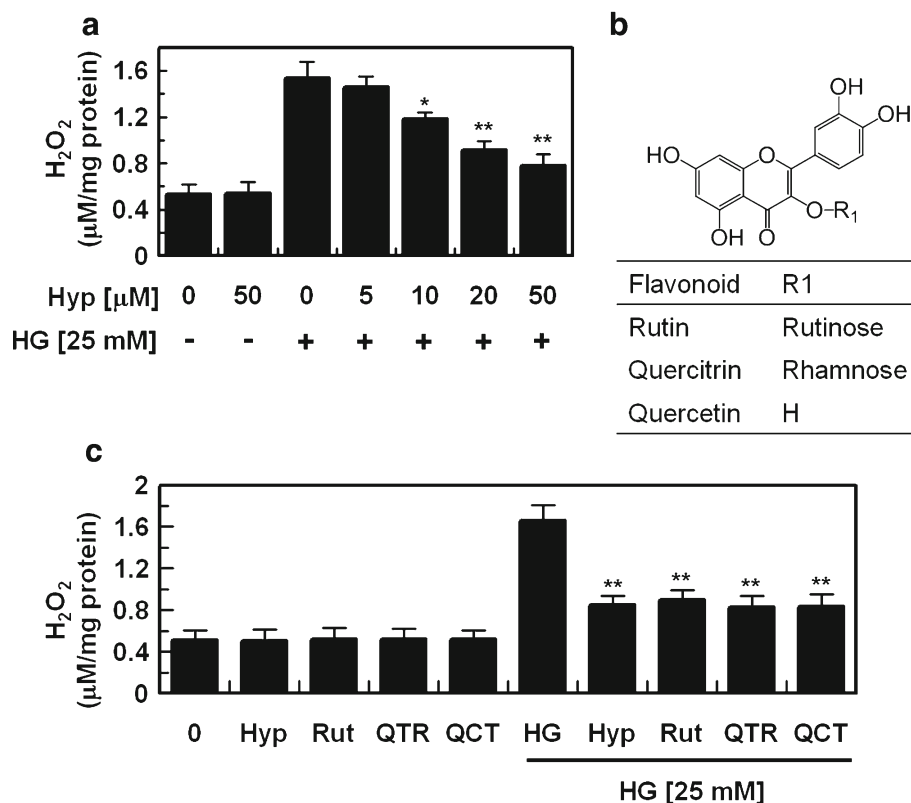


Fig. 5. Effects of hyperoside on HG-induced ROS formation. **a** Cells were pretreated with hyperoside (0–50 μM) for 6 h and then stimulated with HG for 1 h; H₂O₂ assay was then performed as described in the “Materials and Methods” section. **b** Structures of rutin (*Rut*), quercitrin (*QTR*), or quercetin (*QCT*). **c** The same as Fig. 5a except that cells were pretreated with hyperoside (*Hyp*), rutin (*Rut*), quercitrin (*QTR*), or quercetin (*QCT*) and then stimulated with or without HG (25 mM) for 1 h. Data are expressed as the mean \pm SEM of three independent experiments. $*p < 0.05$ and $**p < 0.01$ versus HG alone.

Effect of Hyperoside on HG-Induced Oxidative Stress

Inflammatory responses have been mechanistically linked to the production of reactive oxygen species (ROS) [41]. Previous observations have indicated that hyperglycemia triggers generation of free radicals, and oxidant stress in various cell types and ROS are considered to be important mediators of several biologic responses, including cell proliferation and extracellular matrix deposition [42, 43]. Therefore, to examine the protective effect of hyperoside in HG-induced oxidative stress, we measured the effect of HG on cellular H₂O₂ concentration. The H₂O₂ level showed a statistically significant increase after incubation for 10 min with 25 mM glucose, and a maximal increase was observed at 1 h (data not shown). Thus, we chose to determine cellular ROS 1 h after glucose treatment in subsequent experiments. As shown in Fig. 5a, pretreatment with 10, 20, and 50 μM hyperoside resulted in significantly inhibited HG-induced H₂O₂ level. In addition, hyperoside itself did not induce

oxidative stress (Fig. 5a), which suggested the importance of HG-induced oxidative stress from HUVECs in determining the character of diabetic complication as well as vascular inflammation.

It is well known that the flavonoids with a catechol group in the B-ring such as hyperoside, rutin, quercitrin, or quercetin (Fig. 5b) have an antioxidant activity [44, 45]. Therefore, we determined the effects of these flavonoids on HG-induced H₂O₂ level. As shown in Fig. 5c, the antioxidant effects of hyperoside were similar to those of rutin, quercitrin, or quercetin, indicating that a common catechol grouping in the B-ring is important in the antioxidant activity against HG-induced ROS formation.

Effect of Hyperoside on HG-Induced Activation of NF-κB

Activation of transcription factors such as NF-κB is known to affect CAMs and to induce a coordinated

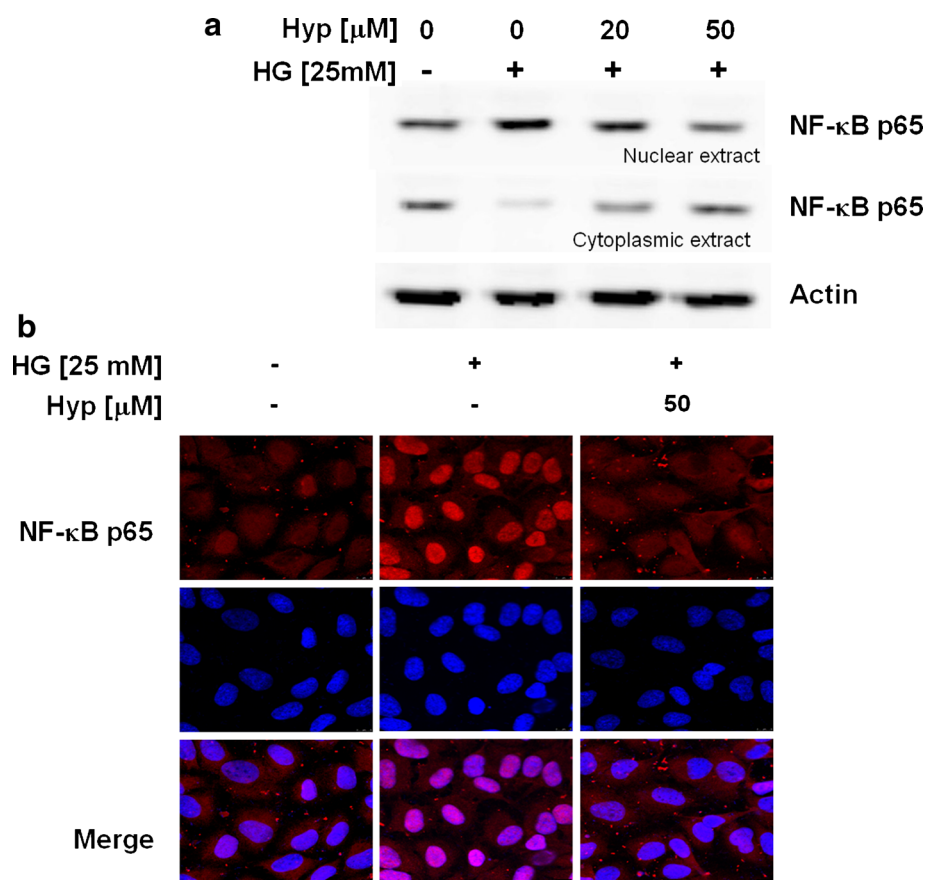


Fig. 6. Effects of hyperoside on HG-induced activation of NF-κB. **a** Cells were pretreated with hyperoside (0, 20, or 50 μM) for 6 h and then stimulated with HG for 1 h. **b** NF-κB p65 was visualized using rabbit anti-p65 monoclonal antibody (1:100), which only recognized NF-κB p65. Goat anti-rabbit antibody (1:100) conjugated to FITC was performed. The subcellular localization of NF-κB p65 was examined by immunofluorescence staining and visualized under an immunofluorescence microscope. The images are representative of the results from three independent experiments.

upregulation of other pro-inflammatory cytokines and chemoattractants, which possibly provides the molecular link between cell redox state and endothelial cell dysfunction [46]. In addition, ROS has been shown to activate various transcription factors, including NF- κ B in cultured endothelial cells [47]. First, we measured HG-induced translocation of NF- κ B from cytosol to nucleus. In Western blotting analysis for determination of NF- κ B p65 protein level, the active subunit of the NF- κ B complex, an increase in the level of the p65 protein, was observed in the nuclear extracts of HUVECs treated with HG, and the cytosolic extracts exhibited an appreciable loss of p65 protein content (Fig. 6a). In addition, pretreatment with hyperoside resulted in inhibition of the HG-induced increase of p65 NF- κ B expression levels (Fig. 6a). To confirm consistency with the result of Western blotting, immunocytochemistry was performed using p65 NF- κ B and fluorescein isothiocyanate (FITC)-conjugated antibody. As a result, HG induced an increase in the expression of p65 NF- κ B in the nucleus, whereas normal condition did not. In addition, treatment with 50 μ M hyperoside resulted in a decrease in HG-induced expression of p65 NF- κ B in the nucleus. These results were consistent with those of Western blotting (Fig. 6a), demonstrating that HG-induced activation of NF- κ B was inhibited by hyperoside, indicating that hyperoside has some inhibitory effect on the NF- κ B pathways specific to HG-induced adhesion molecules in HUVECs.

Flavonoids possess many biochemical properties, but the best described property of almost every group of flavonoids is their capacity to act as antioxidants [44, 45]. The configuration, substitution, and total number of hydroxyl groups substantially influence several mechanisms of antioxidant activity such as radical scavenging and metal ion chelation ability [48, 49]. The B-ring hydroxyl configuration is the most significant determinant of scavenging of ROS because it donates hydrogen and an electron to hydroxyl, peroxy, and peroxy nitrite radicals, stabilizing them and giving rise to a relatively stable flavonoid radical [44, 45, 50]. Functional hydroxyl groups in flavonoids mediate their antioxidant effects by scavenging free radicals and/or by chelating metal ions [51]. The chelation of metals could be crucial in the prevention of radical generation which damages target biomolecules [52]. Because of their capacity to chelate metal ions (iron, copper, etc.), flavonoids also inhibit free radical generation [53]. A 3', 4'-catechol structure in the B-ring firmly enhances inhibition of lipid peroxidation. This trait of flavonoids makes them the most effective scavengers of peroxy, superoxide, and peroxy nitrite radicals [48]. Because of oxidation the B-ring of flavonoids having catechol group, a fairly stable

orthoquinone radical is formed which is a strong scavenger. Flavones lacking catechol system on oxidation lead to the formation of unstable radicals that exhibit weak scavenging potential [54]. Therefore, the antioxidant effects of hyperoside against HG-induced ROS formation (Fig. 5c) may be dependent on the catechol group in the B-ring because the antioxidant effects of hyperoside were similar to those of rutin, quercitrin, or quercetin which have a common catechol grouping in the B-ring.

In summary, our results demonstrate that treatment with hyperoside resulted in blockade of HG-induced vascular inflammation via inhibition of NF- κ B in primary human endothelial cells. These results suggest that hyperoside has significant therapeutic benefits against diabetic complications and atherosclerosis by attenuating HG-induced generation of H₂O₂, increased activation of NF- κ B, upregulation of adhesion molecules, and monocyte-endothelial adhesion and disruption of the endothelial barrier function. Our findings indicate that hyperoside can be regarded as a candidate for use in the treatment of diabetic vascular inflammatory diseases.

ACKNOWLEDGMENTS

This study was supported by the National Research Foundation of Korea (NRF) funded by the Korean government [MSIP] (Grant No. 2013-067053).

Conflict of Interest. The authors declare no conflicts of interest.

REFERENCES

1. Whiting, D.R., L. Guariguata, C. Weil, and J. Shaw. 2011. IDF diabetes atlas: global estimates of the prevalence of diabetes for 2011 and 2030. *Diabetes Research and Clinical Practice* 94: 311–321.
2. Grundy, S.M., I.J. Benjamin, G.L. Burke, et al. 1999. Diabetes and cardiovascular disease: a statement for healthcare professionals from the American Heart Association. *Circulation* 100: 1134–1146.
3. Thomas, J.E., and J.M. Foody. 2007. The pathophysiology of cardiovascular disease in diabetes mellitus and the future of therapy. *Journal of the Cardiometabolic Syndrome* 2: 108–113.
4. Roglic, G., N. Unwin, P.H. Bennett, et al. 2005. The burden of mortality attributable to diabetes: realistic estimates for the year 2000. *Diabetes Care* 28: 2130–2135.
5. Rubino, F., and M. Gagner. 2002. Potential of surgery for curing type 2 diabetes mellitus. *Annals of Surgery* 236: 554–559.
6. Holman, R., and R. Turner. 1991. Oral Agents and Insulin. *Textbook of Diabetes* 462–476.
7. Li, G.Q., A. Kam, K.H. Wong, et al. 2012. Herbal medicines for the management of diabetes. *Advances in Experimental Medicine and Biology* 771: 396–413.

8. Day, C. 1998. Traditional plant treatments for diabetes mellitus: pharmaceutical foods. *British Journal of Nutrition* 80: 5–6.
9. Aggarwal, B.B., H. Ichikawa, P. Garodia, et al. 2006. From traditional Ayurvedic medicine to modern medicine: identification of therapeutic targets for suppression of inflammation and cancer. *Expert Opinion on Therapeutic Targets* 10: 87–118.
10. Bae, J.S. 2012. Role of high mobility group box 1 in inflammatory disease: focus on sepsis. *Archives of Pharmacol Research* 35: 1511–1523.
11. Middleton Jr., E., and G. Drzewiecki. 1984. Flavonoid inhibition of human basophil histamine release stimulated by various agents. *Biochemical Pharmacology* 33: 3333–3338.
12. Mukaida, N. 2000. Interleukin-8: an expanding universe beyond neutrophil chemotaxis and activation. *International Journal of Hematology* 72: 391–398.
13. Hirano, T., S. Higa, J. Arimitsu, et al. 2006. Luteolin, a flavonoid, inhibits AP-1 activation by basophils. *Biochemical and Biophysical Research Communications* 340: 1–7.
14. Zou, Y., Y. Lu, and D. Wei. 2004. Antioxidant activity of a flavonoid-rich extract of *Hypericum perforatum* L. in vitro. *Journal of Agricultural and Food Chemistry* 52: 5032–5039.
15. Zhou, W., J. Oh, W. Li, D.W. Kim, S.H. Lee, and M. Na. 2013. Phytochemical studies of Korean endangered plants: a new flavone from *Rhododendron brachycarpum* G. Don. *Bulletin of the Korean Chemical Society* 34: 2535–2538.
16. Verma, N., G. Amresh, P.K. Sahu, N. Mishra, V. Rao Ch, and A.P. Singh. 2013. Pharmacological evaluation of hyperin for antihyperglycemic activity and effect on lipid profile in diabetic rats. *Indian Journal of Experimental Biology* 51: 65–72.
17. Li, F.R., F.X. Yu, S.T. Yao, Y.H. Si, W. Zhang, and L.L. Gao. 2012. Hyperin extracted from Manchurian rhododendron leaf induces apoptosis in human endometrial cancer cells through a mitochondrial pathway. *Asian Pacific Journal of Cancer Prevention* 13: 3653–3656.
18. Kim, S.J., J.Y. Um, and J.Y. Lee. 2011. Anti-inflammatory activity of hyperoside through the suppression of nuclear factor- κ B activation in mouse peritoneal macrophages. *American Journal of Chinese Medicine* 39: 171–181.
19. Li, Z.L., J. Hu, Y.L. Li, et al. 2013. The effect of hyperoside on the functional recovery of the ischemic/reperfused isolated rat heart: potential involvement of the extracellular signal-regulated kinase 1/2 signaling pathway. *Free Radical Biology and Medicine* 57: 132–140.
20. Ku, S.K., T.H. Kim, S. Lee, S.M. Kim, and J.S. Bae. 2012. Anti-thrombotic and profibrinolytic activities of isorhamnetin-3-O-galactoside and hyperoside. *Food and Chemical Toxicology* 53C: 197–204.
21. Lee, W., S.K. Ku, and J.S. Bae. 2013. Emodin-6-O-beta-D-glucoside down-regulates endothelial protein C receptor shedding. *Archives of Pharmacol Research* 36: 1160–1165.
22. Bae, J.S., and A.R. Rezaie. 2013. Thrombin inhibits HMGB1-mediated proinflammatory signaling responses when endothelial protein C receptor is occupied by its natural ligand. *BMB Reports* 46: 544–549.
23. Bae, J.S., W. Lee, and A.R. Rezaie. 2012. Polyphosphate elicits proinflammatory responses that are counteracted by activated protein C in both cellular and animal models. *Journal of Thrombosis and Haemostasis* 10: 1145–1151.
24. Lee, J.D., J.E. Huh, G. Jeon, et al. 2009. Flavonol-rich RVHxR from *Rhus verniciflua* Stokes and its major compound fisetin inhibits inflammation-related cytokines and angiogenic factor in rheumatoid arthritic fibroblast-like synovial cells and in vivo models. *International Immunopharmacology* 9: 268–276.
25. Akeson, A.L., and C.W. Woods. 1993. A fluorometric assay for the quantitation of cell adherence to endothelial cells. *Journal of Immunological Methods* 163: 181–185.
26. Kim, I., S.O. Moon, S.H. Kim, H.J. Kim, Y.S. Koh, and G.Y. Koh. 2001. Vascular endothelial growth factor expression of intercellular adhesion molecule 1 (ICAM-1), vascular cell adhesion molecule 1 (VCAM-1), and E-selectin through nuclear factor-kappa B activation in endothelial cells. *Journal of Biological Chemistry* 276: 7614–7620.
27. Mackman, N., K. Brand, and T.S. Edgington. 1991. Lipopolysaccharide-mediated transcriptional activation of the human tissue factor gene in THP-1 monocytic cells requires both activator protein 1 and nuclear factor kappa B binding sites. *Journal of Experimental Medicine* 174: 1517–1526.
28. Laakso, M. 1999. Hyperglycemia and cardiovascular disease in type 2 diabetes. *Diabetes* 48: 937–942.
29. Kannel, W.B., and D.L. McGee. 1979. Diabetes and cardiovascular disease. The Framingham study. *JAMA* 241: 2035–2038.
30. Nannipieri, M., L. Rizzo, A. Rapuano, A. Pilo, G. Penno, and R. Navalesi. 1995. Increased transcapillary escape rate of albumin in microalbuminuric type II diabetic patients. *Diabetes Care* 18: 1–9.
31. Wardle, E.N. 1994. Vascular permeability in diabetics and implications for therapy. *Diabetes Research and Clinical Practice* 23: 135–139.
32. Tooke, J.E. 1995. Microvascular function in human diabetes. A physiological perspective. *Diabetes* 44: 721–726.
33. Gerrity, R.G. 1981. The role of the monocyte in atherogenesis. I. Transition of blood-borne monocytes into foam cells in fatty lesions. *American Journal of Pathology* 103: 181–190.
34. Esposito, C., G. Fasoli, A.R. Plati, et al. 2001. Long-term exposure to high glucose up-regulates VCAM-induced endothelial cell adhesiveness to PBMC. *Kidney International* 59: 1842–1849.
35. Hamuro, M., J. Polan, M. Natarajan, and S. Mohan. 2002. High glucose induced nuclear factor kappa B mediated inhibition of endothelial cell migration. *Atherosclerosis* 162: 277–287.
36. Morigi, M., S. Angioletti, B. Imberti, et al. 1998. Leukocyte-endothelial interaction is augmented by high glucose concentrations and hyperglycemia in a NF- κ B-dependent fashion. *Journal of Clinical Investigation* 101: 1905–1915.
37. Lopes-Virella, M.F., and G. Virella. 1992. Immune mechanisms of atherosclerosis in diabetes mellitus. *Diabetes* 41(Suppl 2): 86–91.
38. Kado, S., T. Wakatsuki, M. Yamamoto, and N. Nagata. 2001. Expression of intercellular adhesion molecule-1 induced by high glucose concentrations in human aortic endothelial cells. *Life Sciences* 68: 727–737.
39. Hansson, G.K., and P. Libby. 2006. The immune response in atherosclerosis: a double-edged sword. *Nature Reviews Immunology* 6: 508–519.
40. Boisvert, W.A. 2004. Modulation of atherogenesis by chemokines. *Trends in Cardiovascular Medicine* 14: 161–165.
41. Inoguchi, T., P. Li, F. Umeda, et al. 2000. High glucose level and free fatty acid stimulate reactive oxygen species production through protein kinase C—dependent activation of NAD(P)H oxidase in cultured vascular cells. *Diabetes* 49: 1939–1945.
42. Dunlop, M. 2000. Aldose reductase and the role of the polyol pathway in diabetic nephropathy. *Kidney International. Supplement* 77: S3–S12.
43. Han, H.J., Y.J. Lee, S.H. Park, J.H. Lee, and M. Taub. 2005. High glucose-induced oxidative stress inhibits Na⁺/glucose cotransporter activity in renal proximal tubule cells. *American Journal of Physiology. Renal Physiology* 288: F988–F996.
44. van Acker, S.A., D.J. van den Berg, M.N. Tromp, et al. 1996. Structural aspects of antioxidant activity of flavonoids. *Free Radical Biology and Medicine* 20: 331–342.
45. Rice-Evans, C.A., N.J. Miller, and G. Paganga. 1996. Structure-antioxidant activity relationships of flavonoids and phenolic acids. *Free Radical Biology and Medicine* 20: 933–956.
46. Rimbach, G., G. Valacchi, R. Canali, and F. Virgili. 2000. Macrophages stimulated with IFN-gamma activate NF-kappa B and induce MCP-1 gene expression in primary human endothelial cells. *Molecular Cell Biology Research Communications* 3: 238–242.
47. Uemura, S., H. Matsushita, W. Li, et al. 2001. Diabetes mellitus enhances vascular matrix metalloproteinase activity: role of oxidative stress. *Circulation Research* 88: 1291–1298.
48. Heim, K.E., A.R. Tagliaferro, and D.J. Bobilya. 2002. Flavonoid antioxidants: chemistry, metabolism and structure-activity relationships. *Journal of Nutrition and Biochemistry* 13: 572–584.

49. Pandey, A.K., A.K. Mishra, and A. Mishra. 2012. Antifungal and antioxidative potential of oil and extracts derived from leaves of Indian spice plant *Cinnamomum tamala*. *Cell Mol Biol (Noisy-le-grand)* 58: 142–147.
50. Cao, G., E. Sofic, and R.L. Prior. 1997. Antioxidant and prooxidant behavior of flavonoids: structure-activity relationships. *Free Radical Biology and Medicine* 22: 749–760.
51. Kumar, S., A. Mishra, and A.K. Pandey. 2013. Antioxidant mediated protective effect of *Parthenium hysterophorus* against oxidative damage using in vitro models. *BMC Complementary and Alternative Medicine* 13: 120.
52. Leopoldini, M., N. Russo, S. Chiodo, and M. Toscano. 2006. Iron chelation by the powerful antioxidant flavonoid quercetin. *Journal of Agricultural and Food Chemistry* 54: 6343–6351.
53. Brown, J.E., H. Khodr, R.C. Hider, and C.A. Rice-Evans. 1998. Structural dependence of flavonoid interactions with Cu^{2+} ions: implications for their antioxidant properties. *Biochemical Journal* 330(Pt 3): 1173–1178.
54. Sekher Pannala, A., T.S. Chan, P.J. O'Brien, and C.A. Rice-Evans. 2001. Flavonoid B-ring chemistry and antioxidant activity: fast reaction kinetics. *Biochemical and Biophysical Research Communications* 282: 1161–1168.